

Manuscript Number:

Title: Comparison of the Annealing Behaviour between cold and warm rolled ELC steels by Thermoelectric Power Measurements

Article Type: Full Length Article

Section/Category:

Keywords: ferritic steels; precipitation; recrystallisation; rolling; thermoelectric power

Corresponding Author: Juan Pablo Ferrer,

Corresponding Author's Institution: CENIM-CSIC

First Author: Juan Pablo Ferrer

Order of Authors: Juan Pablo Ferrer; Tommy De Cock; Carlos Capdevila; Francisca García Caballero; Carlos García de Andrés

Manuscript Region of Origin:

Abstract: Abstract

The variations of thermoelectric power (TEP) measurements during annealing of warm and cold rolled extra low carbon (ELC) steels were analysed. Where a prominent influence of recovery was detected in cold rolled steels during annealing, almost no variation of TEP due to both recovery and recrystallisation was observed during annealing of warm rolled steels. On the other hand, TEP measurements were proven to be a powerful technique to monitor dissolution of cementite and precipitation of aluminium nitrides. It was found that these two phenomena significantly affect TEP measurements and recrystallisation kinetics during annealing of warm rolled steels.

Figure 1  
[Click here to download high resolution image](#)

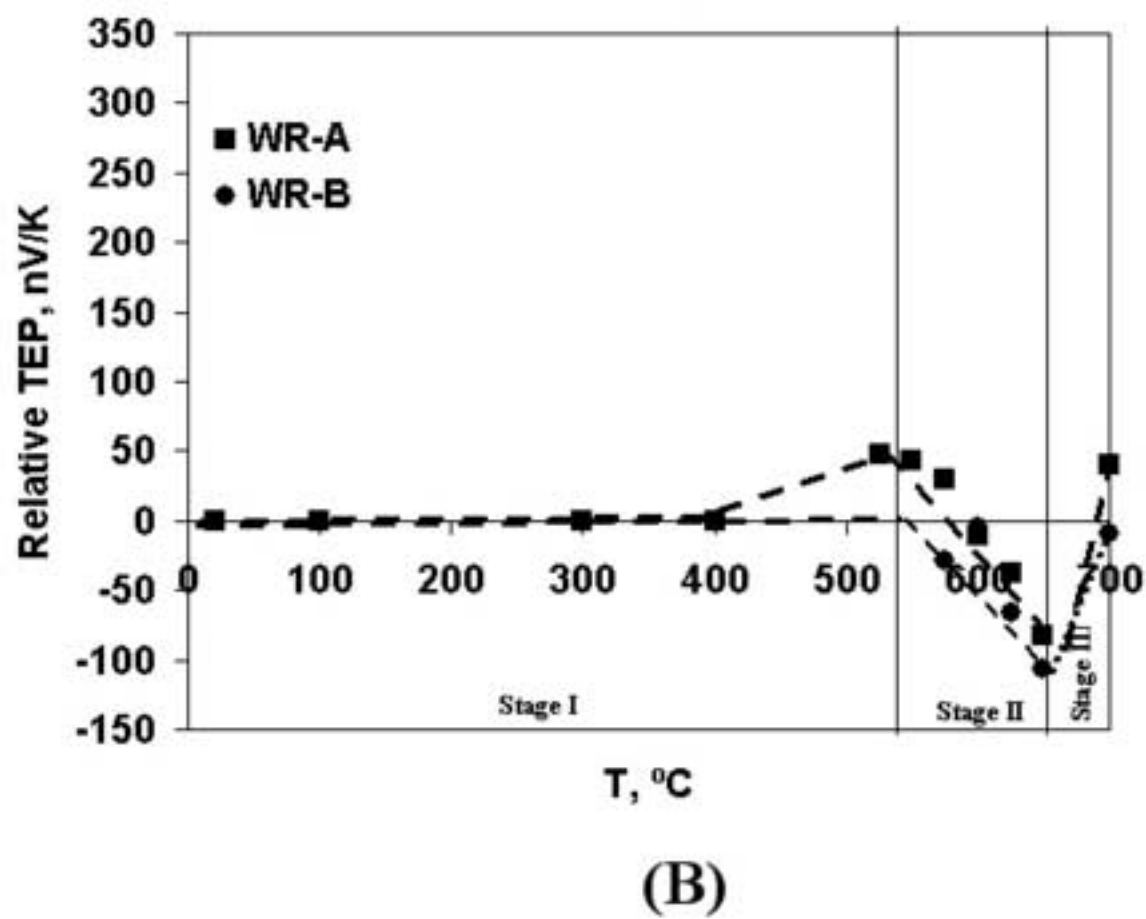
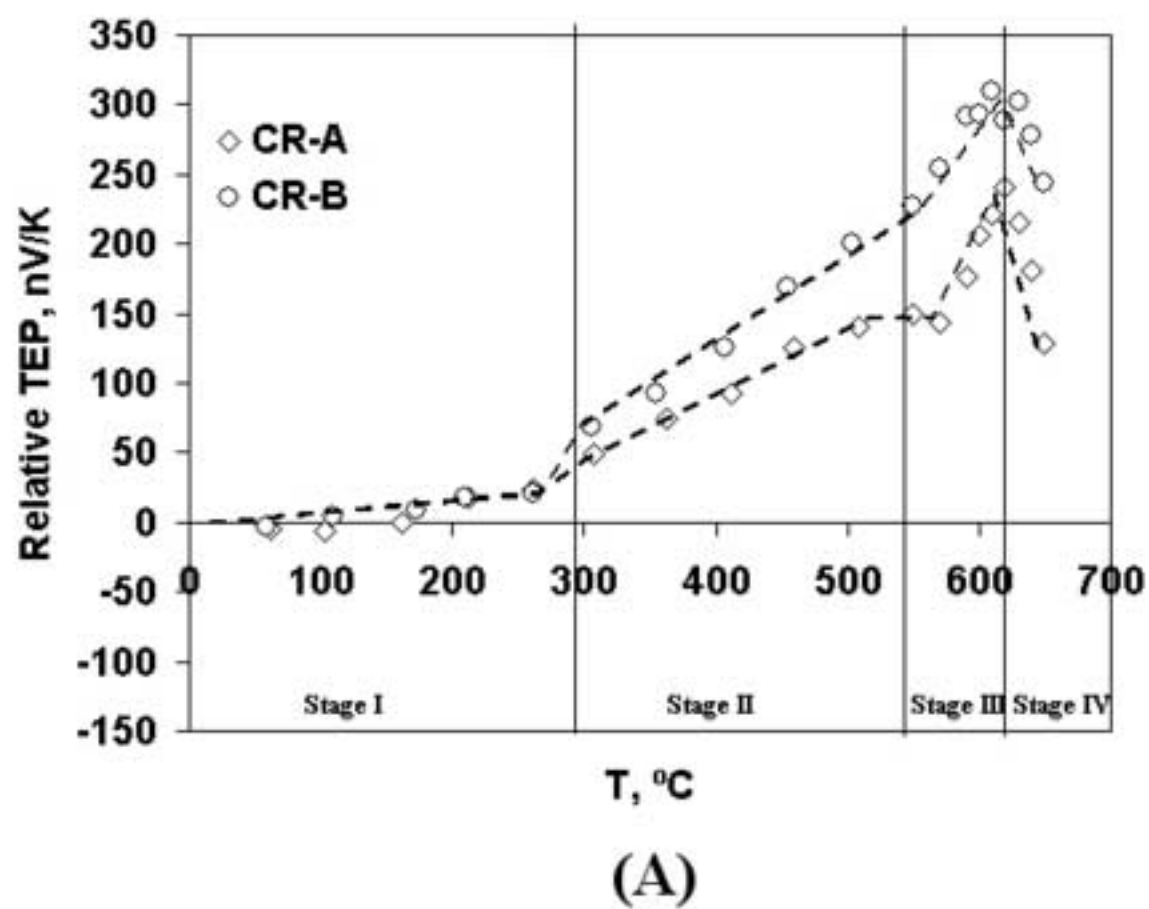


Figure 2  
[Click here to download high resolution image](#)

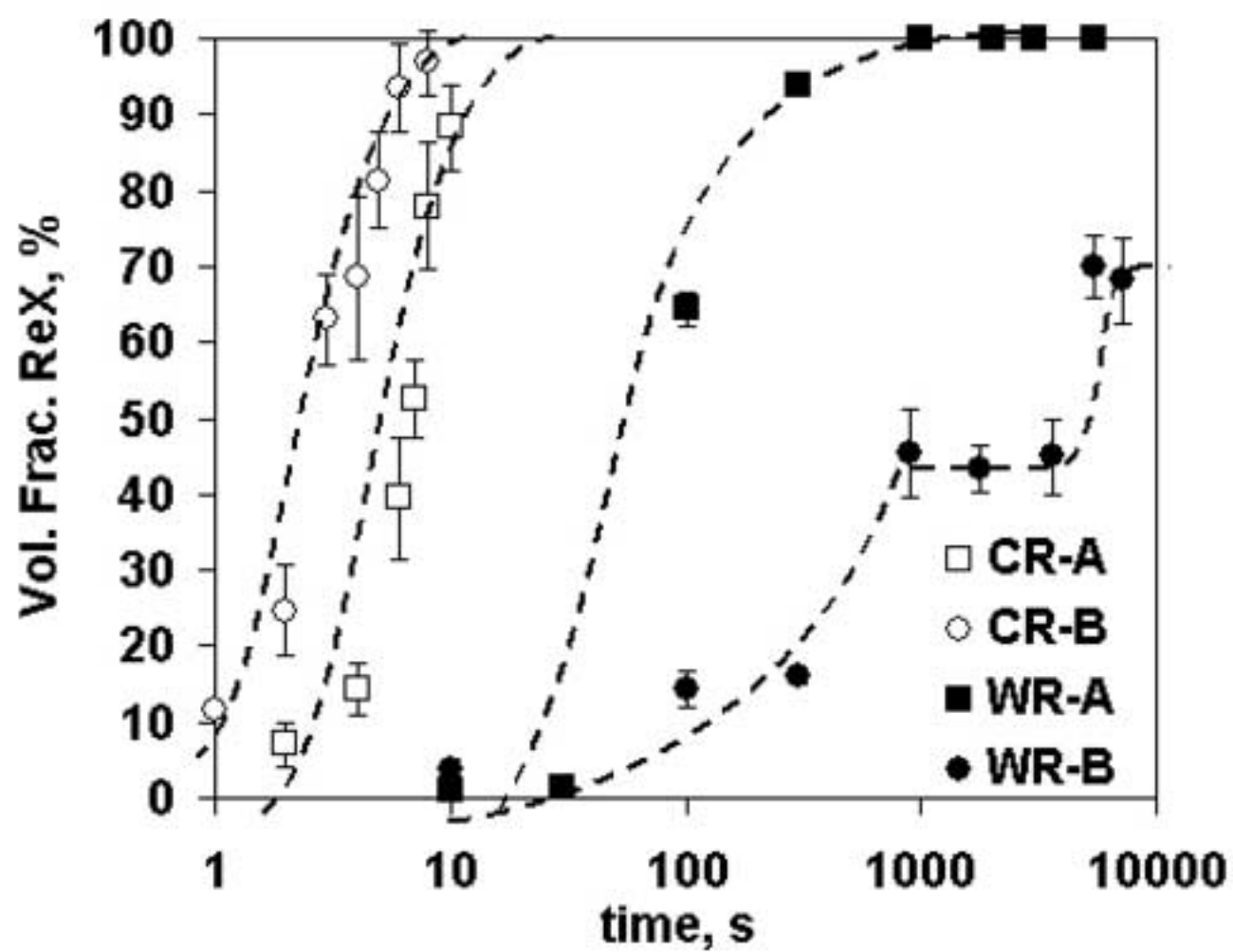
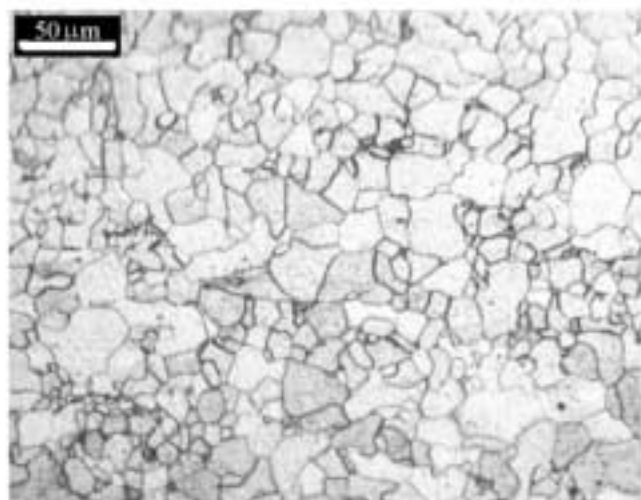
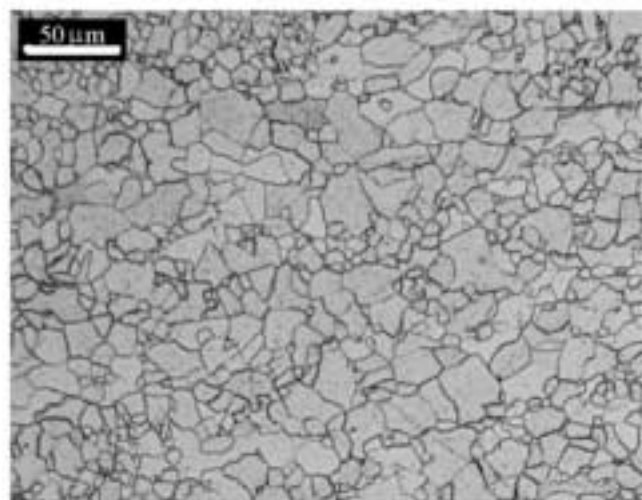


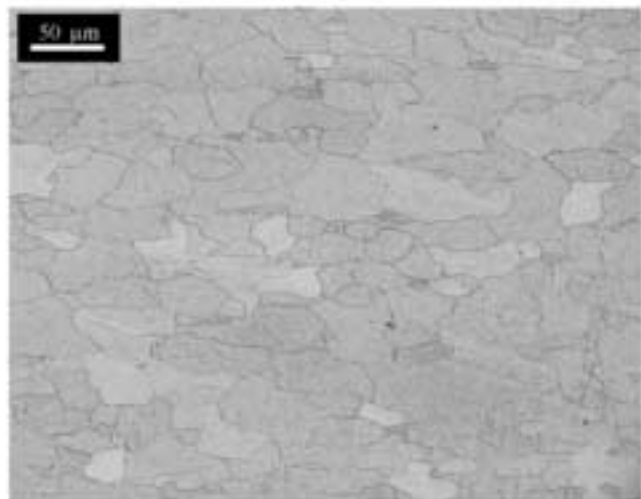
Figure 3  
[Click here to download high resolution image](#)



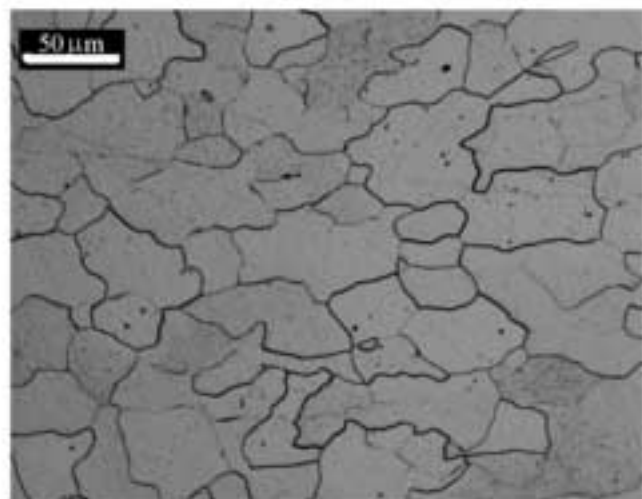
(A)



(B)



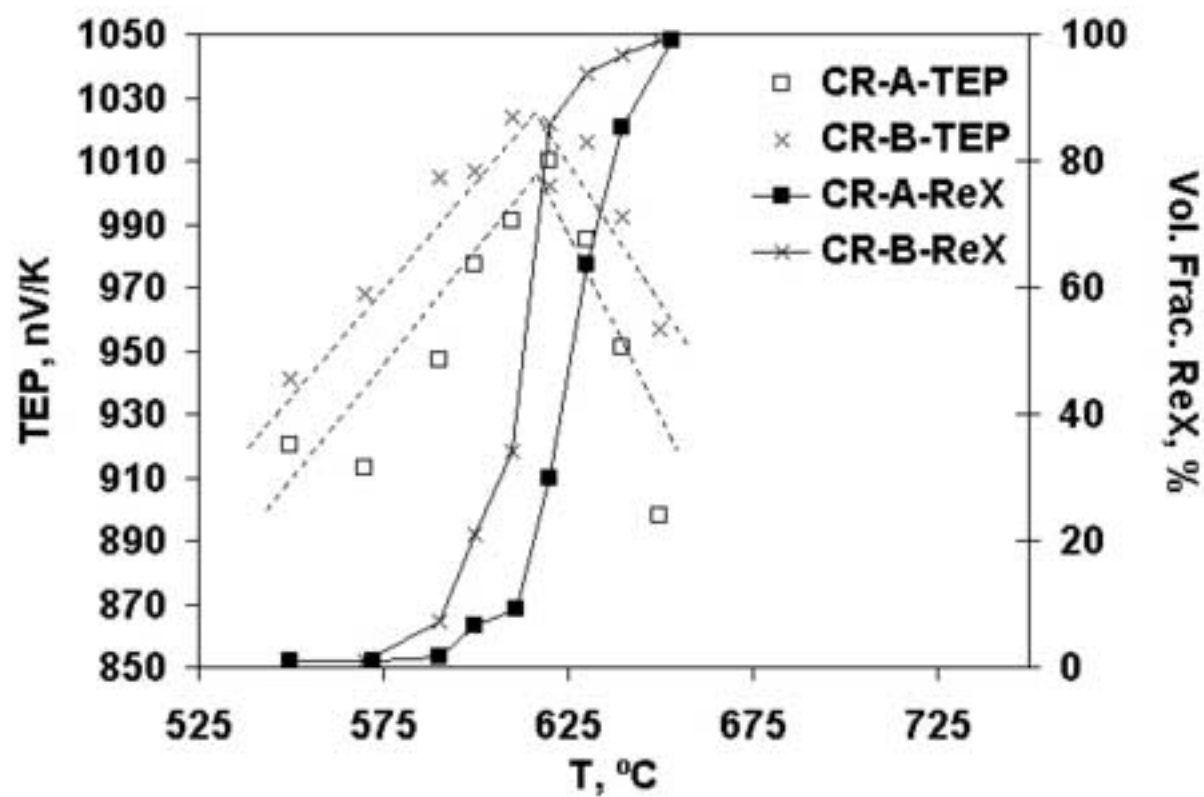
(C)



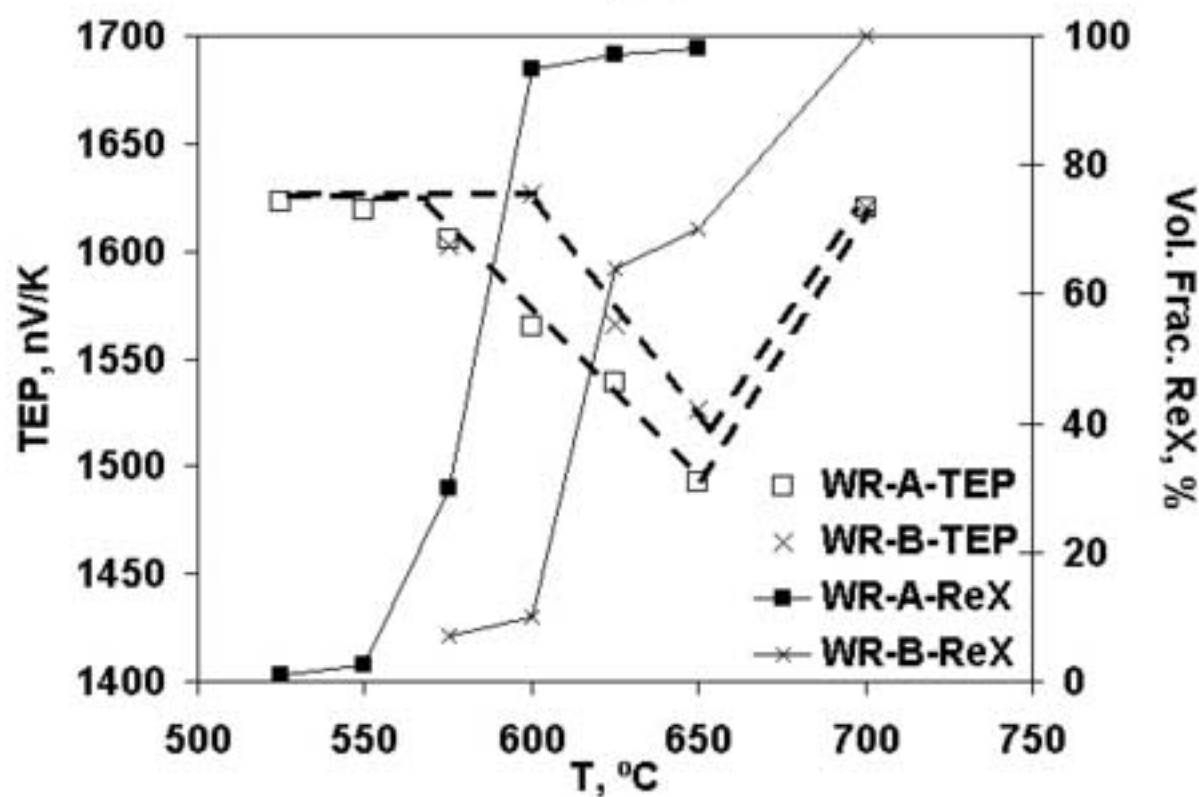
(D)

Figure 4

[Click here to download high resolution image](#)



(A)



(B)

Figure 5  
[Click here to download high resolution image](#)

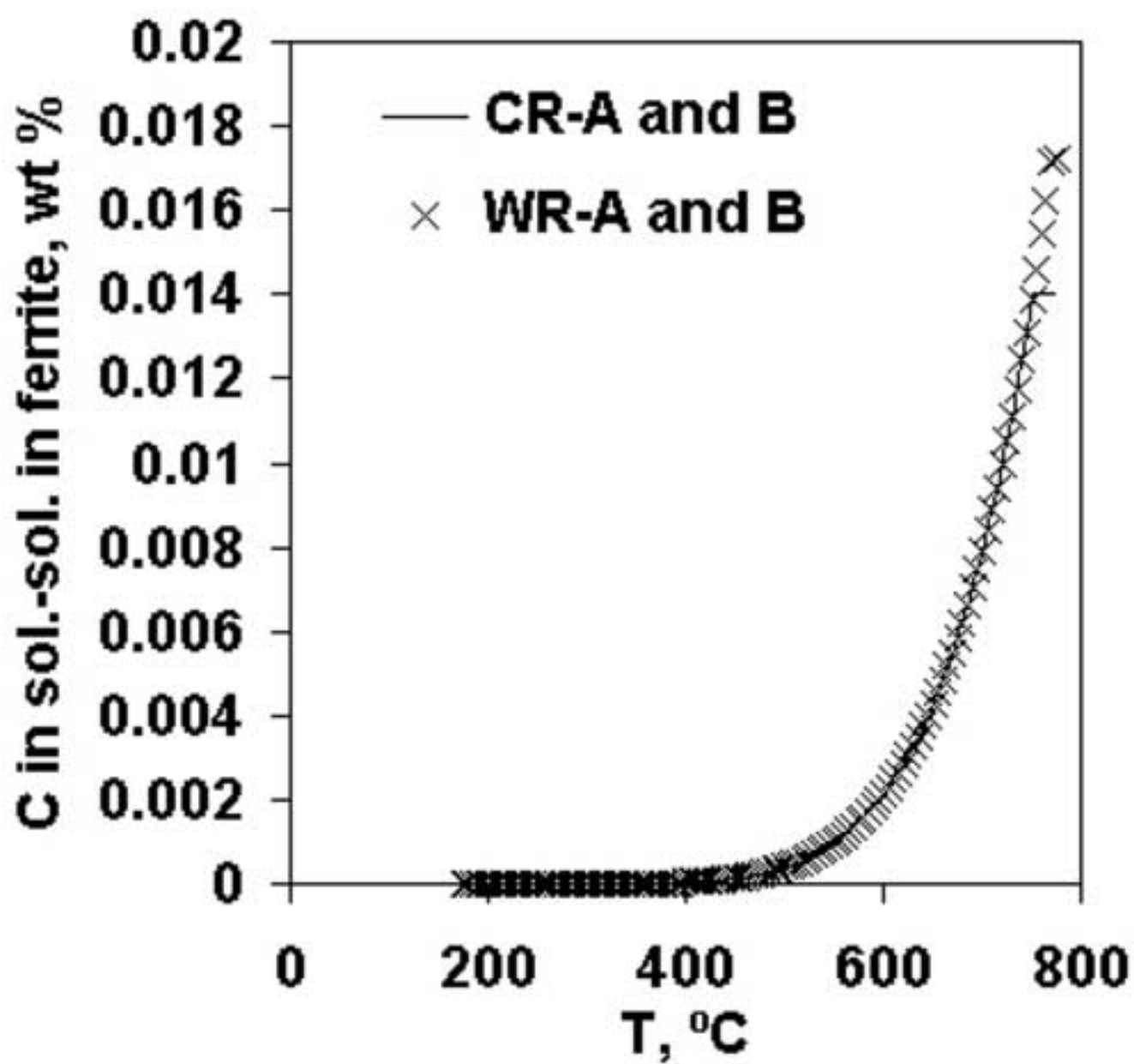
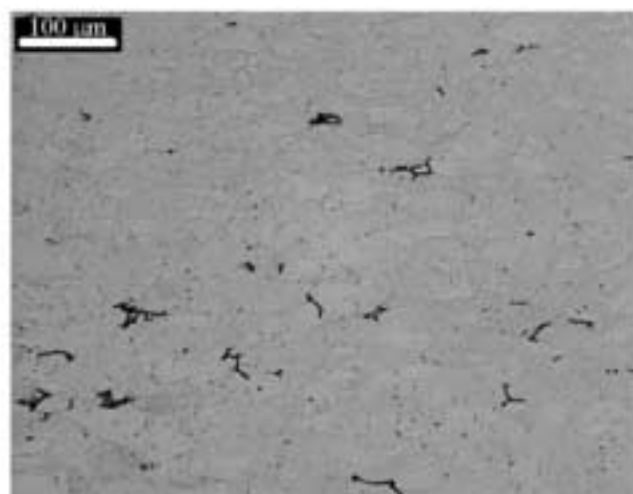
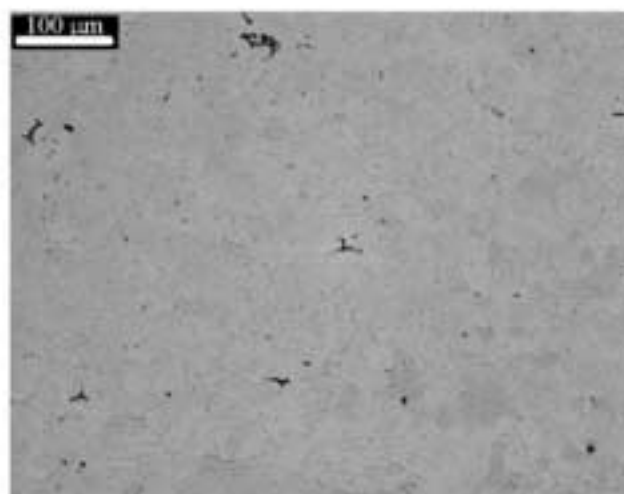


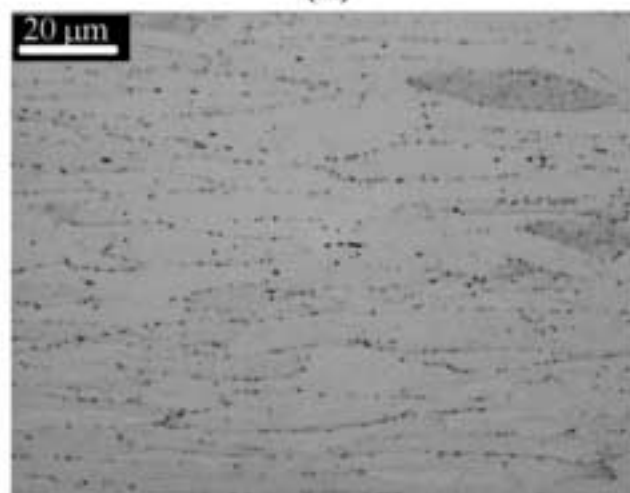
**Figure 6**  
[Click here to download high resolution image](#)



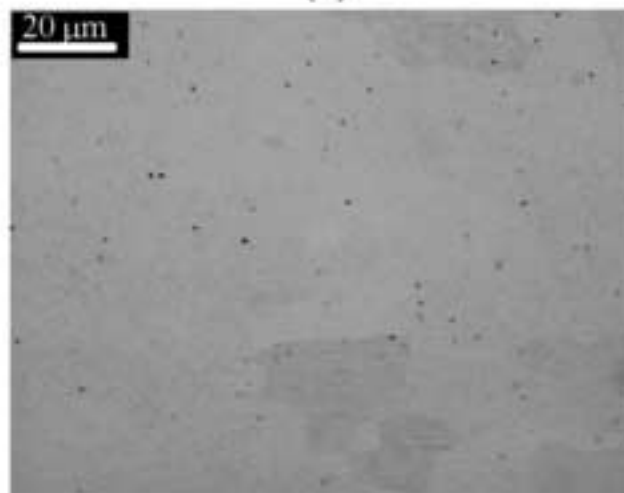
**(A)**



**(B)**



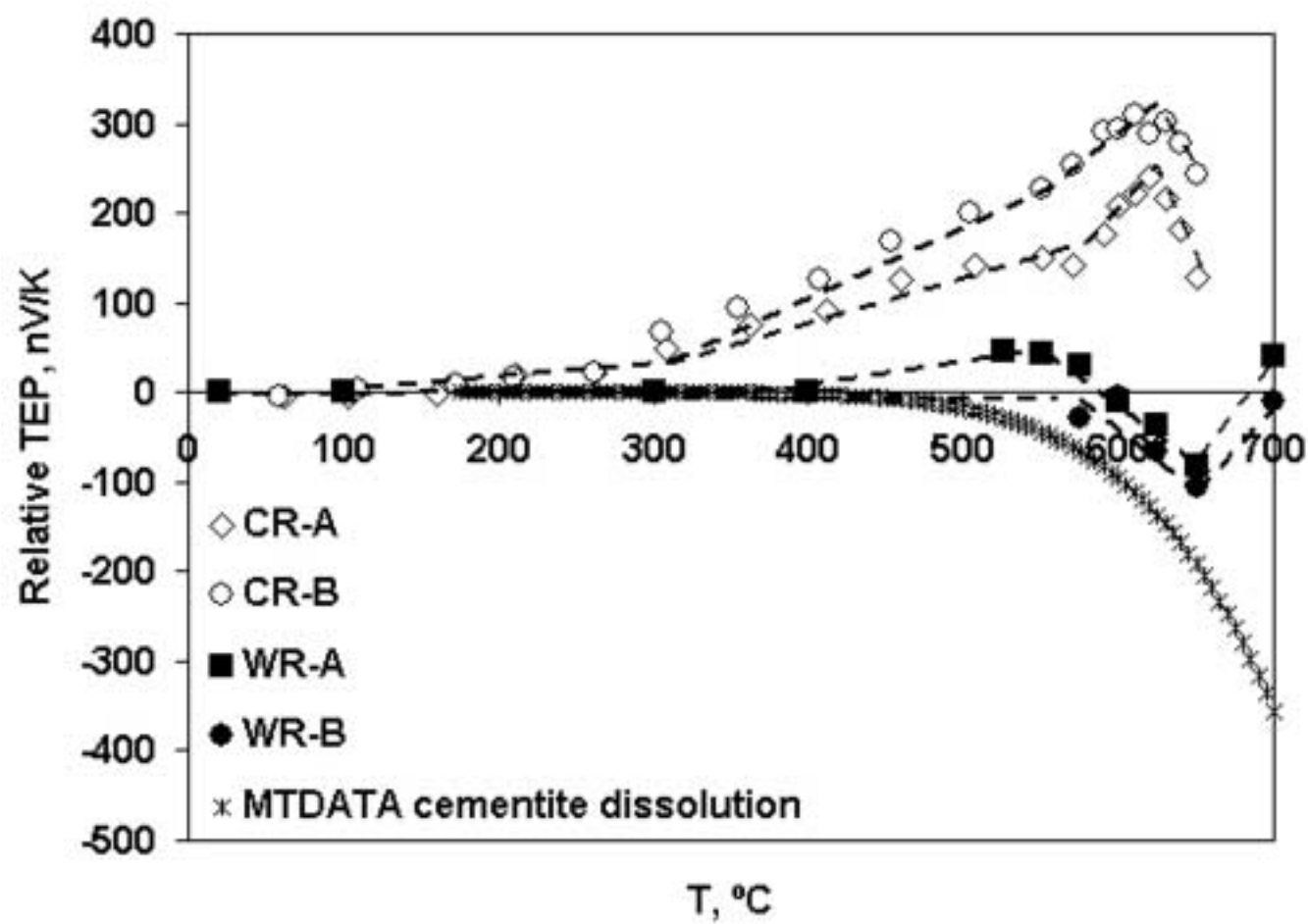
**(C)**



**(D)**

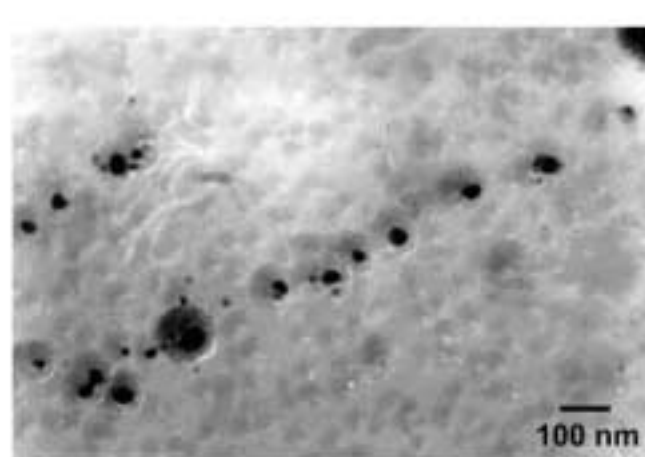


Figure 7  
[Click here to download high resolution image](#)

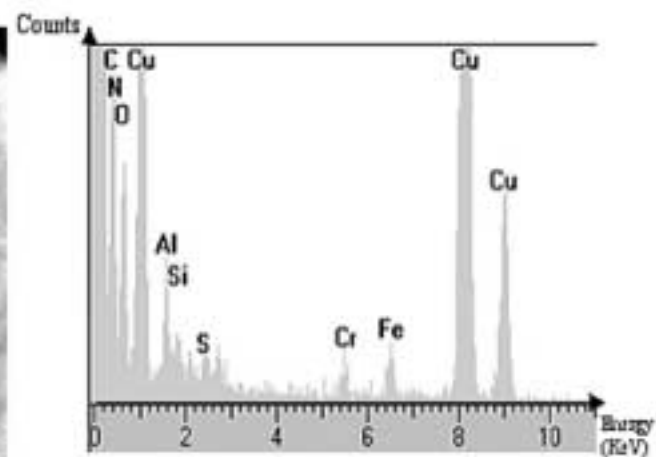




**Figure 8**  
[Click here to download high resolution image](#)



**(A)**



**(B)**

Figure 9  
[Click here to download high resolution image](#)

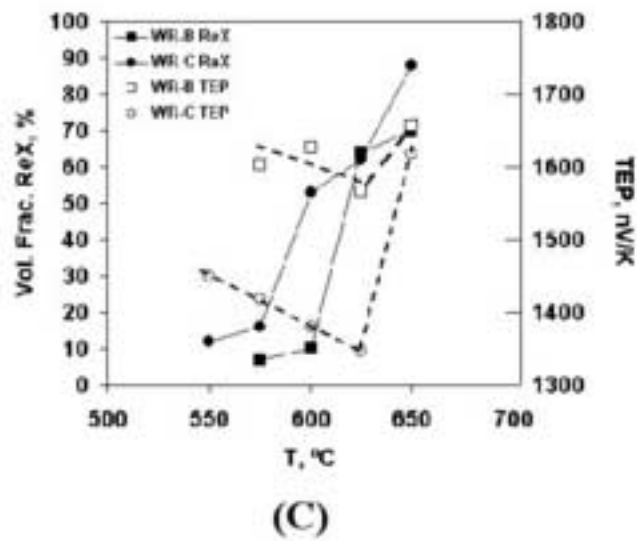
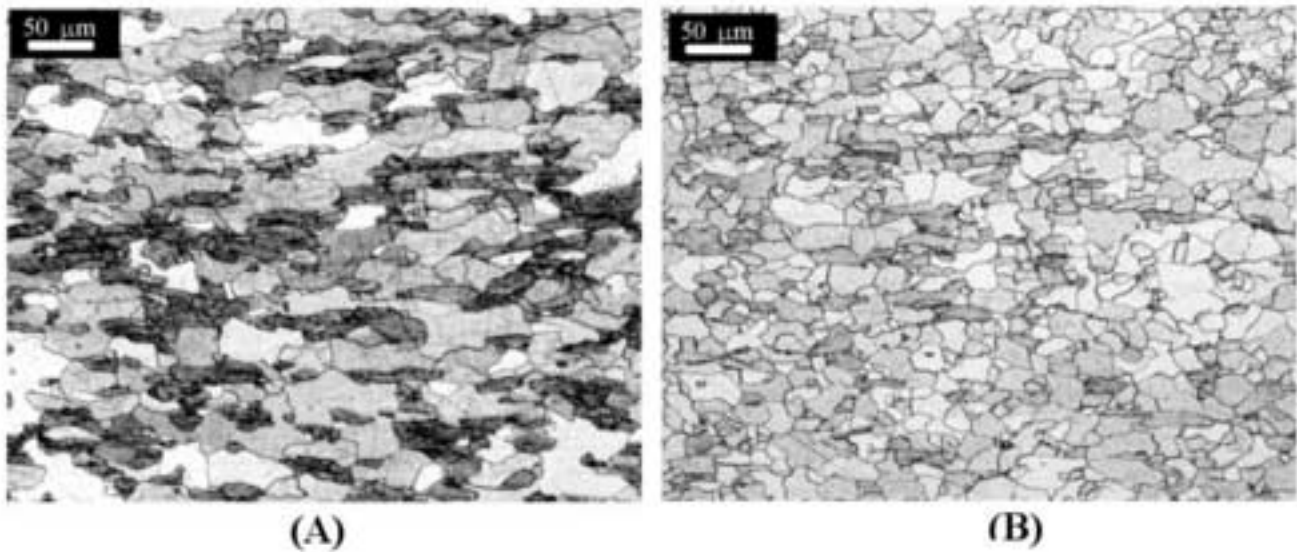


Figure 10  
[Click here to download high resolution image](#)

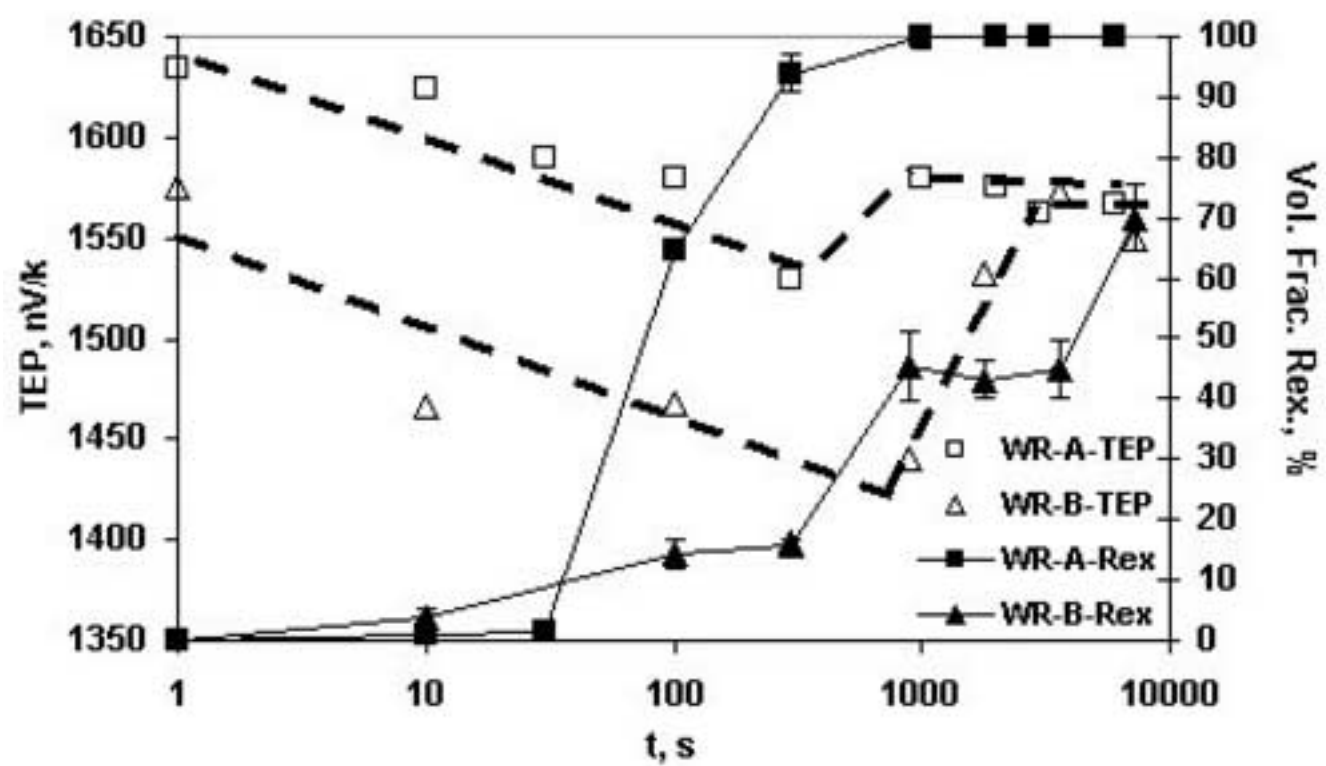


Figure 1. TEP evolution with annealing temperature in (a) CR steels, and (b) in WR steels.

Figure 2. Evolution of the volume fraction of recrystallisation with time during annealing at 650 °C.

Figure 3. Recrystallised samples (a) CR-A, and (b) CR-B, both at 650 °C, (c) WR-A at 625°C, and (d) WR-B at 700 °C. (2% Nital etching).

Figure 4. Evolution of TEP measurements and recrystallised volume fraction with annealing temperature in (a) CR and (b) WR steels.

Figure 5. Carbon in solid solution in ferrite calculated by using MTDATA.

Figure 6. Optical micrographs of samples (a) CR-A annealed at 640 °C, (b) CR-A at 680 °C, (c) WR-A at 575 °C, and (d) WR-A at 625 °C.

Figure 7. Evolution of TEP with annealing temperature and evolution due to dissolution of cementite according to MTDATA

Figure 8. (a) Alignment of AlN precipitates on WR-B steel and (b) XEDS spectrum

Figure 9. Microstructure of (a) WR-B and (b) WR-C both after annealing 1.5h at 650°C, and (c) evolution of TEP and recrystallised fraction with annealing temperature (holding time of 1.5h).

Figure 10. Evolution of recrystallised fraction and TEP on annealing at 650°C in samples WR-A and WR-B.

## Introduction

Warm rolling of low carbon steel sheets is nowadays more and more accepted as a low cost substitute for the conventional cold rolled and annealed sheets. Because of the high temperature drop in the finishing mill and the lower deformation resistance of ferrite, the warm rolling practice below the  $\gamma \rightarrow \alpha$  transformation is the most suitable processing way for rolling thinner gauges of low carbon steels [1-3]. The warm rolling schedule may play a prominent role during the subsequent recrystallisation that, in a similar manner to the cold rolled product, is the last metallurgical process to impact the final properties.

The increase of deformation temperature during warm rolling as compared with cold rolling enhances the diffusion of atoms and increases the equilibrium level of solute carbon. These are manifested as an enhancement of dynamic recovery, AlN precipitation and strain ageing [1-2]. Both dynamic recovery and AlN precipitation reduce nucleation density of strain-free grains and slow down recrystallisation kinetics during a subsequent annealing, since dynamic recovery involves the annihilation of dislocations during deformation, and AlN precipitates pin the growing recrystallised grains [4]. Strain ageing occurs when interstitial atoms such as N and C segregate to dislocations during deformation. It has been previously reported that the removal of C and N from solid solution has a beneficial effect on the recrystallisation texture desirable for deep drawing applications [5-6].

Numerous studies revealed that TEP is a powerful method to monitor microstructural changes such as recovery, recrystallisation and dissolution-precipitation processes in steels [7-12]. This technique is very sensitive to the amount of atoms in solid solution [12-14]. In this sense, this work was aimed at increasing the current understanding of recrystallisation after cold and warm rolling, with reference to the effect of dissolution and precipitation of second phase particles, through the interpretation of TEP measurements.

## Materials and Experimental Procedure

The chemical composition of the investigated steels is listed in Table I. Cold (CR) and warm (WR) rolled steels were subjected to a typical hot-rolling process. CR steels were then air-cooled down to the coiling temperatures listed in Table I. Finally, cold rolling took place at room temperature (RT) with the corresponding reductions listed in Table I. On the other hand, WR steels were air cooled to the warm rolling temperature and deformed according to the parameters listed in Table I. After rolling, the steels were immediately water quenched to prevent further static recrystallisation, in order to preserve the as-rolled microstructure to the greatest possible extent.

**Table I. Chemical composition (in wt.-%) and processing parameters of the studied steels.**

	C	Si	Mn	P	S	Al	Ti	N	Coil*	WRT**	Red***
CR-A	0.014	0.007	0.19	0.007	0.016	0.055	0.001	0.0025	740	-	60
CR-B	0.014	0.007	0.19	0.007	0.016	0.055	0.001	0.0025	740	-	80
WR-A	0.030	0.005	0.17	0.009	0.006	0.041	0	0.0030	-	630	66
WR-B	0.030	0.005	0.17	0.009	0.006	0.041	0	0.0030	-	630	56
WR-C	0.030	0.005	0.17	0.009	0.006	0.041	0	0.0030	-	530	55

\*Coil = Coiling Temperature in °C

\*\*WRT = Warm Rolling Temperature in °C

\*\*\*Red = Reduction in thickness in %

CR and WR steels were annealed at temperatures ranging from 100 °C to 700 °C for different times up to 5400 s before gas quenching. The heating rate selected for annealing experiments was 20 °C/s. Microstructural changes during annealing were followed by means of thermoelectric power (TEP) measurements. A schematic representation of the TEP apparatus is given elsewhere [8]. The experimental procedure of the TEP measurement is the following: the sample is pressed between two blocks of a reference metal (in this case, aged plain carbon steel). One of the blocks is at 15 °C, while the other is at 25 °C to obtain a temperature difference  $\Delta T$ . A potential difference  $\Delta V$  is generated at the reference metal contacts. The apparatus does not give the absolute TEP value of the sample, but a relative TEP ( $\Delta S$ ) in comparison to the TEP of the aged plain carbon steel at 20 °C. Finally, metallographic examination was carried out using conventional methods.

In this work, most of the discussion takes place by comparing results of CR-A and WR-A steels. CR-B and WR-B steels are only used to analyse the effect of cold and warm deformation on recrystallisation, respectively. Finally, a comparison between WR-A and WR-C will allow to conclude about the role of warm rolling temperature on recrystallisation.

The thermodynamic calculations involved have been performed using the commercial software package developed by National Physics Laboratory (NPL) and called MTDATA [15]. The evolution of carbon in solid solution into ferrite with temperature and cementite precipitation has been calculated with this software.

## Results and Discussion

Figure 1 shows the evolution of TEP measurements along the temperature interval between RT and 700 °C. The holding time at each temperature is 10 s for CR steels, and 1.5 h for WR steels. The criterion to define the length of the isothermal hold was the minimum time to detect a few recrystallised grains at 550 °C in the reference steels, *i.e.* CR-A and WR-A for cold and warm rolled steels, respectively.

To follow the effect of annealing on a specific material it is convenient to use a relative TEP scale with this material as the reference level. Thus, the TEP value corresponding to the as-cold rolled state for CR steels, and the water quenched state for WR steels, *i.e.* 770 and 714 nV/K for CR-A and CR-B steels, and 1576 and 1632 nV/K for WR-A and WR-B steels, were chosen as the reference level.

It is clear from the figure that four stages may be differentiated during annealing of CR steels, and only three for WR steels. Each stage is determined by a slope change of the TEP curve. In the case of the CR steels the first stage corresponds to temperatures ranging from RT to 300 °C, the second between 300 and 550 °C, the third between 550 and 625 °C, and the last stage is situated at temperatures above 625 °C. Regarding WR steels the first stage corresponds to temperatures between RT and 550 °C, the second between 550 and 650 °C and finally the third stage is situated above 650 °C.

It is well known that in steels recovery takes place at temperatures ranging from 350 to 500 °C [16], but as seen in Figure 1, an increase of the TEP value is observed at temperatures below 300 °C, where no recovery is expected. Therefore, only segregation to dislocation of interstitial elements, N and C, is expected at these temperatures. In order to separate the TEP contribution of segregation from recovery-recrystallisation, an ageing treatment at 270 °C for 1.5h was performed on the two CR steels. The TEP variation measured between the cold rolled state and the aged state was 100 nV/K, and this value was associated with the segregation of the free interstitial atoms of the steel to the dislocations [17-18]. Moreover, a slope change can be distinguished in TEP variation in Figure 1 around 300 °C for CR steels, which is probably related to the transition between strain ageing and recovery processes.

On the other hand, it has been reported elsewhere that bcc metals such as ferrite experience recovery when they are subjected to deformation at high temperatures [19-21]. This means that, on the contrary to cold rolled sheets, the overall effect on the TEP of recovery during annealing of warm rolled sheets is rather small. Furthermore, in WR steels no changes of TEP were observed during annealing at temperatures below 400 °C neither. This suggests that dynamic strain ageing has occurred during warm rolling itself, causing the interstitial atoms such as C and N to diffuse towards the dislocations. This means that no dislocations and/or interstitial atoms are available for a subsequent strain ageing during annealing and in this way no variation of the TEP value is recorded. Therefore, Stage I corresponds to the strain ageing effect for the CR steels, whereas no equivalent was found in the WR steels. Concerning the effect of dislocations on the TEP measurements, it has been clearly established that cold working, *i.e.* the introduction of dislocations, leads to a negative TEP variations [14]. Therefore, since recrystallisation is not observed at temperatures below 550 °C, the increase of TEP in the second stage (see Figure 1 (a)) is due to recovery processes.

It is also clear from Figure 1 that a higher deformation in the initial state leads to a more pronounced rise of the TEP measurements during recrystallisation. Likewise, it is also observed that the influence of recovery on TEP measurements in WR steels is almost negligible as compared with that in CR steels. Whereas no significant increase of the TEP measurements is detected in WR steels up to 500 °C, a substantial increase of TEP is detected in CR steels between 300 and 500 °C. Therefore, Stage II in CR steels and Stage I in WR steels correspond to recovery processes.

On the other hand, it must be remarked that recrystallisation in WR steel is considerably more sluggish than in CR steels, as is reflected by the different holding time at each annealing temperature. From Figure 2 it is inferred that the holding time to obtain a given amount of recrystallisation at an annealing temperature of 650 °C increases by approximately 2-3 orders of magnitude in WR steels as compared with CR steels. However, both cold and warm rolled steels follow the same tendency, *i.e.* the increase of deformation during the rolling processes accelerates recrystallisation. This leads to coarser recrystallised grains in WR than in CR steels, which is consistent with the recrystallised microstructures shown in Figure 3. Metallographic examination of fully recrystallised samples shows that the microstructure of CR steels consists of well equiaxed recrystallised grains, whereas in WR steels the grains are more anisotropic in shape, elongated along the rolling direction. Another important observation involves the apparent inhibition of recrystallisation in the WR-B steel. This will be analysed later on.

Figure 4 shows the evolution of TEP and the recrystallised volume fraction with annealing temperature for two different levels of deformation during the cold and warm rolling process. In the CR steel, TEP values range from 910 to 1020 nV/K, whereas in the WR steels these values are between 1500 and 1850 nV/K. This difference is due to the higher amount of elements in solid solution (see Table I). Previous works revealed the strong influence of elements in solid solution on TEP, because they create new diffusion centers for electrons and phonons [12], and it was concluded that increasing amounts of elements in solid solution, even in a small amount, can significantly decrease TEP [20-21]. Furthermore, precipitation and/or dissolution of precipitates lead to changes in the amount of atoms in solid solution and therefore to variations of the TEP [11].

Beside the difference between the nominal values of TEP in both types of steel, there is also a remarkable contrast in their tendency, as can be noted in Figure 4(a).

In the CR steels an increase of the TEP with increasing temperature is observed, until at 625 °C the values start to decrease (Figure 4(a)). In WR steels a steady decrease of the TEP for increasing temperatures is detected, followed by a sudden rise at 700 °C (Figure 4(b)). Neither strain ageing nor the recovery and recrystallisation processes are able to explain this evolution. Hence, an additional effect must take place simultaneously during the



anneal in both types of steel. A close observation of the experimental results permits the assumption that the precipitation and dissolution of particles constitute the additional contribution to TEP in the considered temperature intervals. Indeed, the precipitation of incoherent second phase particles such as cementite and AlN has an important influence on the TEP values [14], since this process causes an impoverishment of solute elements in the ferrite matrix and consequently increases TEP. Vice versa the dissolution of precipitates provokes a decrease of TEP, due to the enrichment of the ferrite. Therefore, it is reasonable to consider that Stage III in CR steels corresponds to recrystallisation, whereas Stage IV is related with the dissolution of precipitates. On the other hand, the decrease of TEP at temperatures ranging from 550 to 650 °C in WR steels (Stage II) could be due to the dissolution of precipitates, while the sudden increase of the TEP at annealing temperatures above 650 °C could be provoked by precipitation processes (Stage III). These hypotheses will be demonstrated further on.

The comparison between recrystallisation and TEP in CR steels Figure 4(a) and Figure 1(a)) shows that most of the increase of TEP occurs before any recrystallisation takes place. It is therefore clear from this data that the TEP is highly sensitive to the recovery process and in less extent to recrystallisation effects.

So far the influence that recovery and recrystallisation have on the TEP evolution in CR and WR steels has been studied. In the following sections the influence of precipitation – dissolution process will be analysed.

In the high annealing temperature regime, *i.e.* above 600 °C, it is possible to disclose a common pattern between warm and cold rolled steels. The decrease of the TEP in all steels for temperatures above 600 °C may be explained by cementite dissolution. Data provided by MTDATA (Figure 5) show how the amount of carbon in equilibrium in solid solution increases with annealing temperature.

As is shown in Figure 6, the metallographic examination of CR and WR samples etched with picral (4% picric acid plus 96% ethanol) shows the gradual dissolution of cementite particles as the temperature increases. Therefore the increase of carbon in solid solution into ferrite predicted by MTDATA arises from the dissolution of cementite.

The variation of the TEP value due to a change of carbon concentration ( $[C]$ ) can be expressed as follows:

$$\Delta S^{rel} = K_C [C] \quad (1)$$

where  $\Delta S^{rel}$  is the relative TEP value between the as-quenched sample after deformation process and the annealed sample,  $[C]$  is the carbon concentration in wt.-%, and  $K_C$  is the TEP constant for carbon in solid solution for which a value of -45000 nV/K(wt.-%) has been proposed [21].

Figure 7 shows the expected evolution of  $\Delta S^{rel}$  according to these calculations. It can be seen that a good correlation between experimental and calculated results exists during annealing between 550 and 650 °C for both CR and WR steels, without considering the prominent effect of recovery in the CR steels (Stage III). The comparison between Figure 4(a), Figure 7 and Figure 1 suggests that the decrease of the TEP at high temperatures is probably due to cementite dissolution in CR and WR steels. However, a clear discrepancy is observed for temperatures above 650 °C in WR steels (Stage III). While theoretical calculations predict a significant drop of the TEP, experimental results revealed that TEP increases. This rise of the TEP could be related to AlN precipitation. In order to study this hypothesis, AlN particles were identified in TEM replicas of the WR-B steel (Figure 8).

The first indication that some precipitation is taking place during annealing in WR steels comes from a close observation of Figure 2. It can be seen that the evolution of the volume fraction of recrystallisation with time in WR-B reaches a plateau. Such inhibition of

recrystallisation is characteristic of the coupling of precipitation and recrystallisation mechanisms [23].

On the other hand, precipitation previous to cold rolling or recovery – recrystallisation processes usually has little influence, but when it occurs during recovery and recrystallisation the second phase provides a resistance to both nucleation and growth of new grains [24-27]. The tendency for AlN precipitation to take place on prior and sub-grain boundaries may provide anisotropic barriers for growth. As a consequence, new grains have an anisotropic shape mainly elongated along the rolling direction (see Figure 2). Likewise, when precipitation takes place during recrystallisation, it will hinder the progress of this process until annealing promotes coarsening of AlN particles. This is consistent with the inhibition of recrystallisation detected in Figure 2 for WR-B, where new grains nucleate and grow until precipitation of AlN takes place. Nevertheless, at the highest annealing temperature (700 °C) most of the recrystallisation takes place before any precipitation events occur. In this case, precipitation has no influence on recrystallisation.

In order to analyse the effect that precipitation exerts on recrystallisation during annealing in WR steels, a new ELC steel (WR-C steel) was submitted to a similar thermomechanical process as WR-A and WR-B, but with a lower warm rolling temperature (530 °C, see Table I). That temperature allows avoiding most of the aluminium precipitation. Subsequently this sample was annealed for 1.5 h at temperatures between 550 and 650 °C.

Figures 9 (a) and (b) show a comparison between the microstructures obtained after 1.5 h at 650 °C in WR-B and WR-C. Whereas the microstructure of WR-B is only partially recrystallised, almost the complete microstructure of WR-C is recrystallised. This fact, together with the observation of more equiaxed and finer recrystallised grains in WR-C (16 µm in WR-C vs. 31 µm in WR-B), allows to conclude that recrystallisation proceeds without hindrance in this steel as compared with WR-B. Likewise, Figure 9(c) shows the changes in TEP and recrystallisation fraction during the 1.5 h annealing at different temperatures. There is a clear difference of the TEP variation, although at 650 °C the same value is reached. This difference may be explained by the AlN precipitation as follows.

According to the Gorter-Nordheim law, the contribution of the elements in solid solution on the TEP of pure iron is given by the following equation [28]:

$$\Delta S_{ss} = \sum_i P_i \times [x_i] \quad (2)$$

In this equation  $[x_i]$  represents the content of the i-th element in solid solution in wt. % and  $P_i$  is the coefficient that reflects the effect of the element on the thermoelectric power of pure iron. The value of  $P_i$  in a certain steel (named steel 1) can be obtained if its value in another steel (named as steel 2) is known, as well as the electrical resistivities of both steels [7]:

$$\frac{P_i^1}{P_i^2} = \frac{\rho_2}{\rho_1} \quad (3)$$

being  $P_i^1$  and  $P_i^2$  the coefficients of the i-th element in the steels 1 and 2, and  $\rho_1$  and  $\rho_2$  their respective electrical resistivities. Regarding AlN precipitation,  $P_{Al}$  and  $P_N$  were calculated by Brahmi et. al.[ 14] being  $P_{Al} = -28 \text{ mV/K} \cdot 10^{-3} \text{ wt.}\%$  and  $P_N = -25 \text{ mV/K} \cdot 10^{-3} \text{ wt.}\%$  in a low carbon steel. Resistivities are calculated according to the empirical relation given by Meyzaud et. al.[29] :

$$\rho(\mu\Omega) = 9.9 + 30.0([C] + [N]) + 6.0[Mn] + 12.0[Si] + 14.0[P] - 10.0[S] + 6.4[Ti] + 13.0[Al] \quad (4)$$

where the concentrations are given in wt.-%. The previous data allow the estimation of the coefficients for Al and N in the ELC steel of the current work, *i.e.*  $P_{Al} = -43$  and  $P_N = 23$  mV/K\* $10^{-3}$  wt.%. Assuming that the whole amount of nitrogen precipitates as AlN, the variation of the TEP that this precipitation induces is  $\Delta S = 315$  nV/k. Therefore, considering that the amount of carbon in solid solution after annealing in WR-B and WR-C are the same, the difference between the minimum and maximum values of the TEP curves observed in WR-B (90 nV/K) and WR-C (273 nV/K) in Figure 9 corresponds to the amount of AlN that precipitates during annealing. Those data indicate that most of the AlN precipitation has been suppressed during the warm rolling in WR-C, and precipitation takes almost exclusively place during annealing.

A close study of these results supports the assumption that AlN precipitation during warm rolling occurs mainly on sub – grain boundaries. Assuming that recrystallisation in these WR steels proceeds with a continuous recrystallisation mechanism [30-31], these precipitates inhibit the movement of sub – grain boundaries and hence recrystallisation is a very sluggish process in this temperature range. Likewise, this assumption explains the irregular morphology of the recrystallised grains in WR-B (see Figure 9(a)) and the equiaxed morphology of WR-C (see Figure 9(b)), as well as the differences of the recrystallised volume fraction observed in Figure 9(c).

If all the AlN particles precipitate during warm rolling, the subsequent recrystallisation proceeds slowly but steadily until full recrystallisation is obtained. However, if some Al and N remain in solid solution after warm rolling, AlN particles precipitate during recrystallisation itself. This leads to an inhibition of recrystallisation, as detected in WR-B (see Figure 2) and which is reflected by a recrystallised microstructure composed of non-equiaxed grains (Figure 9 (a)).

However, one last phenomenon that has to be explained is why two steels with identical composition and warm deformation temperature, WR-A and WR-B, show a different recrystallisation behaviour, since no stagnation of the recrystallisation is observed in steel WR-A (Figure 2). In Figure 10 the evolution of TEP and recrystallised fraction at 650 °C is followed. Firstly, there is a difference in TEP between WR-A and WR-B which remains during the first stages of annealing. This fact is related to the difference in AlN precipitated during warm rolling: as deformation accelerates AlN precipitation [14], less amount of Al and N remains in solid solution in the most deformed steel, *i.e.* WR-A. The first drop in TEP, almost identical in WR-A and WR-B, is due to the dissolution of cementite, as was previously discussed. Longer annealing times promote AlN precipitation. The higher stored energy for recrystallisation in WR-A, because of the higher reduction, accelerates recrystallisation in this steel, which finishes before new AlN precipitation can take place. This avoids the pinning effect during recrystallisation, and hence the recrystallisation of the steel proceeds without an actual stagnation as is the case in steel WR-B. This figure also shows how a prominent increase of TEP and the inhibition of recrystallisation in WR-B coincide. Finally, both WR-A and WR-B reach an identical precipitation state for the longest time denoted by similar TEP values.

## Conclusions

1. TEP has been shown to be a powerful technique to follow the processes that occur during annealing of deformed material. In contrast to other techniques it is highly sensitive to recovery – recrystallisation and dissolution – precipitation processes that take place during annealing.
2. Strain ageing is easily detected in cold rolled steels by TEP measurements. The absence of variations of TEP due to strain ageing in warm rolled steels suggests

- that dynamic strain ageing has occurred during warm rolling, *i.e.* prior to annealing, due to the high temperatures at which warm rolling is performed.
3. During recovery of ELC cold rolled sheets a prominent increase of TEP is observed. Nevertheless, in the case of warm rolling the contribution of this process to TEP is negligible, due to the dynamic recovery.
  4. Recrystallisation of cold rolled material during continuous annealing cycles occurs before dissolution of most of the cementite and precipitation of aluminium nitride. A fully recrystallised and well equiaxed microstructure is developed in a few seconds during annealing in the 600-700 °C temperature range.
  5. When warm rolling is performed at temperatures higher than 600 °C, a severe precipitation of AlN takes place simultaneously during dynamic recovery, which considerably hinders nucleation. This fact, together with the lower stored energy for recrystallisation at higher deformation temperatures, leads to a far lower nucleation density in the warm rolled material than in the cold rolled steel. As recrystallisation progresses, if the amount of deformation is not high enough to provoke a quick recrystallisation, new AlN precipitation events occur during recrystallization which prompt the inhibition of recrystallization.
  6. If warm rolling is performed at lower temperatures, most of the AlN precipitation is prevented during deformation but, depending on the reheating temperature and the amount of deformation, it may precipitate during annealing, before the recrystallization process has finished. Again, AlN may then exert its influence through the inhibition of recrystallisation, until longer reheating times promote coarsening of AlN particles, so that the recrystallisation process may be completed.

### Acknowledgements

The authors acknowledge financial support from European Community and Spanish Ministerio de Educación y Ciencia in the form of ECSC Project (ECSC 7210-PR-351) and a Complementary Project (MAT 2002-10811E). Authors acknowledge T. Iung from Arcelor Reserch (France), G. Lannoo from Centre Recherche Metallurgie (Belgium) and I. Salvatori from Centro Sviluppo di Materiali (Italy) for the fruitful discussions. J.P. Ferrer would like to thank the Spanish Ministerio de Ciencia y Tecnología for the financial support in the form of a FPI Grant and T. De Cock to Consejo Superior Investigaciones Cientificas for the financial support in the form of a I3P Grant.

### References

- [1] Liu D, Humphreys AO, Toroghinezhad MR and Jonas JJ. ISIJ Int 2002; 42: 751-759
- [2] Barnett MR, Jonas JJ and Hodgson PD. 37<sup>th</sup> MWSP Conf Proc ISS, Vol. XXXIII. Warrendale, PA, 1996. pp. 971-978
- [3] Humphreys AO, Liu DS, Toroghinezhad MR and Jonas JJ. ISIJ Int 2002; 42: S52-S56
- [4] Wilson FG and Gladman T. Intern mater rev 1988; 33: 221-285
- [5] Barnett MR and Jonas JJ. ISIJ Int 1999; 39: 856-873
- [6] Senuma T, Yada H, Shimizu R and Harase J. Acta metal et mater 1990; 38: 2673-2681
- [7] Ney JLA. Metall Trans A 1998; 29 : 2669
- [8] Caballero FG, García-Junceda A, Capdevila C and García de Andrés C. Scripta Mater 2005; 52: 501-505

- [9] Lavaire N, Massardier V and Merlin J. Scripta Mater 2004; 50: 131-135
- [10] Kléber X, Borrelly R and Vincent A. La Revue de Métallurgie-CIT/Science et Génie des Matériaux 2001; 201-210
- [11] Lavaire N. Etude des Phénomènes à l'origine du Vieillissement des Aciers pour Emballage à Ultra Bas Carbone (ULC): Apport du Pouvoir Thermoelectrique à la Caractérisation des États Microstructuraux , PhD Thesis, INSA Lyon, 2001.
- [12] Lavaire N, Merlin J and Sardoy V. Scripta mater 2001; 44: 553-559
- [13] Massardier V, Guétaz V, Merlin J and Soler M. Mat Sci Eng, A 2003; 355: 299-310
- [14] Brahmi A and Borrelly R. Acta Mater 1997; 45: 1889-1897
- [15] Metallurgical and Thermochemical Databank, Teddington, Middlessex, National Physical Laboratory, UK, 1996. p.1.
- [16] Humphreys FJ and Hatherly M. In: Recrystallisation and Related Phenomena. Pergamon Press, Oxford, editor. 1995. p.132.
- [17] Cottrell AH, Bilby BA. Proc Phys Soc A 1949; 62:49.
- [18] Soenen B, De AK, Vandeputte S, De Cooman BC. Acta Mater 2004; 52:3483-3492
- [19] Glover G and Sellars CM. Metall Trans 1973; 4: 765-773
- [20] Caballero FG, Capdevila C, Álvarez LF and García de Andrés C. Scripta Mater 2004; 50: 1061-1066
- [21] Caballero FG, García-Junceda A, Capdevila C and García de Andrés C. Scripta Mater 2005; 52: 501-505
- [22] Lavaire N, Merlin J and Sardoy V. Scripta Mater 2001; 44: 553-560
- [23] Zurob HS, Hutchinson CR, Brechet Y and Purdy G. Acta Mater 2002; 50: 3075-3092.
- [24] Michalk JT and Schoone RD. Trans Metall Soc AIME 1968; 242: 1149-1160
- [25] Meyzaud Y and Parnière P. Mémoires et études scientifiques de la revue de métallurgie 1974; 71: 423-434
- [26] Aubrun P and Rocquet P. Mémoires et études scientifiques de la revue de métallurgie 1973; 70: 260-269
- [27] Aubrun P and Rocquet P. Mémoires et études scientifiques de la revue de métallurgie 1973; 70: 275
- [28] Barnard RD. Thermoelectricity in Metals and Alloys. Taylor and Francis, Editors. London, 1972. p. 151.
- [29] Meyzaud Y and Parnière P. Mémoires et études scientifiques de la revue de métallurgie 1974 ; 71: 415-422
- [30] Humphreys FJ and Hatherly M. Recrystallisation and Related Phenomena. Pergamon Press, Oxford, editor. 1995. p.152.

[31] Haldar A and Ray RK. Mat Sci Eng, A 2005; 391: 402-407